Predicting the Unconfined Compressive Strength of Rice Husk Ash – Treated Fine-grained Soils

Rizgar A. Blayi[1], Jamal I. Kakrasul[1†] and Samir M. Hamad[2]

[1]Department of Civil and Environmental Engineering, Faculty of Engineering, Soran University,|
Soran 44008, Kurdistan Region – F.R. Iraq

[2]Scientific Research Centre, Soran University,
Soran, Kurdistan Region – F.R. Iraq

***Abstract*—This study aims to develop novel and accurate data-driven predictive models to replace labor-intensive laboratory testing for estimating the unconfined compressive strength (UCS) of problematic soils treated with rice husk ash (RHA) Full Quadratic, Interaction, M5P-tree, and Artificial Neural Network (ANN) were trained and evaluated using a dataset of 211 samples that involved seven key geotechnical parameters, including RHA content (0–30%), liquid limit (22–108%), plasticity index (1.3–82%), maximum dry density (1.2–1.9 g/cm^3), optimum moisture content (10.5–42.6%), and curing time (CT) (0–112 days). Among all these models, the ANN model demonstrated superior performance (R^2 = 0.97, RMSE = 24 kPa, MAE = 17 kPa, SI = 0.10). Sensitivity analysis revealed CT as the most influence factor (21.9%), followed by moisture content (16.1%) and RHA content (15.3%). The findings present that these predictive models provide a hybrid empirical–machine learning approach, and an accurate alternative to traditional UCS testing, significantly reducing the need for laboratory experiments. They also emphasize enhanced geotechnical performance and the sustainable reuse of agricultural waste. Furthermore, the models can offer a time-efficient solution with practical applications in areas such as highway development and foundation engineering.**

***Index Terms*—Modeling techniques, Rice husk ash stabilization, Soil properties, Unconfined compressive strength prediction**

I. Introduction

Clay soils are among the most common soil types in earthwork projects. These soils are usually susceptible to volume changes, which can cause shrinkage, swelling, and differential settlements (Estabragh, Moghadas, and Javadi, 2013). These volume changes can significantly impact the structural stability of underlying infrastructures such as pavements and foundations. Mechanical and chemical approaches have been used to address problems of clayey soil (Abbey, Eyo and Ng'ambi, 2020; Ahmed, 2013; Blayi, et al., 2024; Lin and Cerato, 2012). Over last decades, integrating industrial and agricultural waste materials (e.g., rice husk ash [RHA]) has gained substantial attention as alternative soil stabilizer, attributable to their sustainability and easy availability (Behak and Musso, 2016; Canakci, Aziz and Celik, 2015; Choobbasti, et al., 2010; Eberemu Adrian, Amadi Agapitus and Sule, 2012). RHA, which is a byproduct of rice milling, is an eco-friendly solid waste material with high amorphous silica content, making it an alternative to traditional soil stabilizers, including cement and lime. Replacing one ton of cement with RHA reduces CO_2 emissions by 0.9 tons, offering a cost-effective and sustainable alternative for geotechnical projects (Khan, et al., 2012; Rahman, 1987).

One of the geotechnical parameters used as a measurement of soil improvement is unconfined compressive strength (UCS). Studies found that the UCS of natural and treated soil can varies with physical properties of soil, including the addition of RHA and other combined agents, the liquid limit (LL), plasticity index (PI), maximum dry density (MDD), optimum moisture content (OMC), and the curing times (CT) (Anwar Hossain Khandaker, 2011; Behak and Musso, 2016; Canakci, Aziz and Celik, 2015; Choobbasti, et al., 2010; Eberemu Adrian, Amadi Agapitus and Sule, 2012; Zivari, Siavoshnia and Rezaei, 2023). In addition, studies have shown that combining RHA with additional stabilizers, including lime, cement, and calcium chloride can further improve soil properties (Ashango and Patra, 2014; Choobbasti, et al., 2010; Maithili, Nagakumar, and Shashishankar, 2024; Pushpakumara and Mendis, 2022). Using RHA as a soil additive not only improves its mechanical properties but also aligns with sustainable development goals by utilizing industrial byproducts to stabilize soil (Ashango and Patra, 2014; Choobbasti et al., 2010; Maithili, Nagakumar, and Shashishankar, 2024; Pushpakumara and Mendis, 2022).

In addition, Free swelling (FS) index, as a measure of soil swelling potential, can complement UCS in evaluating soil stability for predicting soil behavior under varying moisture conditions. Traditional UCS testing is often time-consuming,

ARO-The Scientific Journal of Koya University
Vol. XIII, No. 1 (2025), Article ID: ARO.11967. 14 pages
DOI: 10.14500/aro.11967
Received: 23 December 2024; Accepted: 13 April 2025
Regular research paper; Published: 15 June 2025
†Corresponding author's e-mail: jamal.kakrasul@soran.edu.iq

 http://dx.doi.org/10.14500/aro.11967

labor-intensive, and unusable for large-scale projects. Therefore, studies have explored alternative methods, including predictive modeling to evaluate UCS of soils (Goktepe, et al., 2008; Mawlood et al., 2021 (Mohammed and Vipulanandan, 2015; Mozumder and Laskar, 2015; Mohammed, 2018; Sharma and Singh, 2018; Vipulanandan and Mohammed, 2020). Precise prediction of the UCS is important to obtain the desired improved properties. Soft computing models, including full quadratic (FQ), Interaction (IA), M5P-tree, and ANN models, are commonly used for predicting soil properties. These models can handle difficult conditions in large datasets (Ali, et al., 2024; Mohammed et al., 2021). Recent studies revealed that ANN can be highly effective under certain conditions (Hossain and Kim, 2015; Mozumder and Laskar, 2015; Sharma and Singh, 2018), while FQ, linear, or multilinear regression models may be more suitable in others. Studies use statistical indicators such as R^2, RMSE, MAE, and SI to assess prediction model performance (Mousavi et al., 2011; Westerberg et al., 2015; Zaimoglu, 2015). These measures evaluate the accuracy and reliability of models (Blayi et al., 2021; Baghbani, et al., 2023; Cabalar and Omar, 2023; Baghbani, et al., 2023).

Based on the literature analysis, no prediction models have been developed specifically for estimating the UCS of fine-grain soils treated with RHA. Therefore, this study aims to develop various machine learning and statistical methods to predict the UCS of RHA-treated soil based on easily measurable input parameters (McBratney et al., 2000; Wattanapanich et al., 2024; Zhang et al., 2024). This approach addresses the challenge of conducting geotechnical testing at every site, which can be particularly difficult for small-scale projects. The models investigated include Artificial Neural Networks (ANN), M5P-tree, FQ, and IA models. These models can predict UCS values given sufficient data, relevant input parameters, and a wide range of UCS values. The study employs multiple evaluation techniques to assess the performance and accuracy of each model in predicting UCS for RHA-stabilized soils. ANN models are particularly interesting for their ability to capture complex, nonlinear IAs between material characteristics, stabilization parameters, and performance results, even in high-dimensional data forms. FQ and IA models take IA effects into account when interpreting data, while M5P-tree dividers datasets in an interpretable method. This comparison emphasizes on each model's prediction accuracy and practicality for optimizing RHA content and stabilization strategies. Ultimately, the study presents a novel application of FQ, IA, M5P-tree, and ANN models for predicting the UCS of RHA-stabilized soils, representing a highly accurate, data-driven alternative to traditional labor-intensive and time-consuming testing methods (Emad et al., 2022; Gautam et al., 2023; Nasir Amin et al., 2023).

II. Objectives of the Study

This work aims to develop different models and correlations to predict the UCS of RHA-treated soil utilizing laboratory test results found in the published literature. Four various models, including FQ, IA, M5P-tree, and ANN were developed to predict UCS based on the addition of waste by-product materials and geotechnical properties of the soils. In addition, linear and Vipulanandan model relationships were employed between UCS and FS values. The main objectives of this study are as follows:

1. Develop and compare predictive models to predict the UCS and establish correlations with FS index of the natural and RHA-stabilized soils
2. Evaluate the performance of the models with statistical assessment metrics (R^2, RMSE, MAE, and SI), to identify the most accurate approach
3. Analyze the impact of the additives and soil properties on UCS by conducting a sensitivity analysis to identify the most significant parameters influencing UCS values
4. Establish a sustainable framework for soil improvement by promoting the use of RHA in geotechnical applications and advance the state-of-the-art in geotechnical engineering through AI-driven methods for predicting soil properties.

III. Methodology

This study focuses on developing soft computing and statistical models to predict the UCS of natural and RHA-treated soils and evaluate the impact of other geotechnical properties of soil on UCS values. 211 datasets were collected from various published research and randomly divided into training (70% of data) and testing (30% of data). The training datasets were employed to develop models to predict the UCS values. The models were evaluated using the testing datasets. The retaining 30% for testing assists in defining the model's capacity to generalize to newly introduced data. Moreover, the dataset comprises main geotechnical properties impacting UCS, including RHA content (0–30%), LL (22–108%), PI (1.3–82%), MDD (1.2–1.9 g/cm^3), OMC (10.5–42.6%), and CT (0–112 days). The collected data were preprocessed by removing irregularities and standardizing values to guarantee the best model performance. The models include two learning machine approaches, ANN and M5P-tree, and two statistical regression models: FQ and IA. AI and FQ were chosen for their interpretability, while M5P-tree was included for its ability to combine decision-tree structures with regression. ANN was selected for its capability to capture complex, nonlinear relationships. The ANN architecture consisted of three hidden layers with 64, 32, and 16 neurons, respectively, using ReLU activation.

Table I shows the details of the datasets collected from various studies. The table includes the measured (UCS) kPa ranges, which are compared to the predicted values from the models later. These input parameters were used to develop the models, and their performance was evaluated using the actual values of the output parameters. Fig. 1 shows a flowchart of the study's research approach, which consists of five steps. During the initial stage, data were gathered from numerous sources. In the second stage, input and output parameters were correlated to find potential relationships. In the third stage, the data was divided into two groups: training (70%) and testing (30%). In the fourth stage, models were

TABLE I
THE NUMBER AND THE RANGE OF USED INPUT AND OUTPUT DATASETS

Authors	Data ranges								
	No. data	RHA (%)	Additives (%)	LL (%)	PI (%)	MDD (g/cm³)	OMC (%)	Curing (days)	UCS (kPa)
Rahman (1986)	5	0–16	0	50–53.4	18.2–27.2	1.39–1.56	22–25.7	0	211.2–371.6
Muntohar (2004)	4	0–12.5	0	64–74	25–43	1.18–1.32	34–37.9	0	219–268
Muntohar (2004)	4	0–12.5	6 Lime	54–74	5–23	1.15–1.32	26.5–34	0	238–269
Basha, et al. (2005)	5	0–20	0	35.6–46.5	11.2–14	1.45–1.68	15–24	0	100–140
Alhassan (2008)	1	0	0	49.5	25.1	1.48	18.38	7	180
Murty and Praveen (2008)	5	0–8	0	63–108	32–82	1.50–1.58	24–28.3	0	186–321
Murty and Praveen (2008)	44	0–8	0.25–1 $CaCl_2$	44–76	14–47	1.45–1.61	22–28.5	0–14	181–481
Anwar Hossain Khandaker (2011)	1	0	0	39	19	1.63	21.58	7	94
Yadu, Tripathi and Singh, (2011)	5	6–15	0	52–74	5–10	1.62–1.76	14.4–19.6	0	128–180
Sarkar, et al. (2012)	5	0–12.5	0	46–56	20–24	1.42–1.55	21.4–30.2	0	58–255
Fattah, Rahil and Al-Soudany (2013)	4	0–9	0	56.9–63	28.1–37.2	1.53–1.76	22–25	0	81.9–128.2
Anupam, Kumar and Ransingchung (2014)	1	0	0	46	25	1.68	16.91	7	83.28
Adhikary and Jana (2016)	11	0–20	0	48–63.5	17.8–22	1.29–1.61	20–30.8	0–28	93–235
Kumar Yadav, et al. (2017)	6	0–12.5	0	34.5–36.1	6.2–12.4	1.55–1.64	17–23.3	0	110.9–216.9
Nahar, et al. (2021)	1	0	0	37.5	7.8	1.7	18.7	0	42
Adajar, et al. (2019)	11	0–25	0	48–75	18–53	1.19–1.42	27.3–40.2	7–28	90–320
Jalal, et al. (2021)	35	0–12	0	30.7–36.3	14.6–20.5	1.48–1.7	19.8–26	3–112	75–665
Ordoñez Muñoz, et al. (2021)	14	0–15	2–5 Cement	45.9–51.7	6.9–15	1.34–1.40	25–33	7–90	350–815
Hossain, et al. (2022)	4	0–9	0	35–42	10.5–12	1.56–1.77	15.9–20.1	0	82.7–193.1
Pushpakumara and Mendis (2022)	4	0–20	0	51–66.5	29–33.4	1.37–1.48	26.3–42.6	0	75–87
Pushpakumara and Mendis (2022)	10	0–30	10–20 Lime	38–55	16.5–33	1.23–1.43	26–42	0	79–106
Zivari, Siavoshnia and Rezaei, (2023)	14	0–10	1–4 Lime	22–31.3	1.3–5	1.72–1.84	12.2–16.2	7–28	125–625
Charyulu, et al. (2023)	4	0–15	0–15	63.2–75	34–38	1.3–1.9	22–30	0	72–104
Ingabire and Kumar (2023)	5	0–15	6 Sawdust ash	25–40	10.2–21.1	1.38–1.56	17.8–19.7	0	13.1–24.6
Maithili, Nagakumar and Shashishankar (2024)	3	5–15	5–15	32–35	7.5–16	1.63–1.84	13–16.8	0	92–128
Abdulrahman, et al. (2024)	5	0–10	0–10	55–62	14–41	1.6–1.74	10.5–15	0	65–100

RHA: Rice husk ash, LL: Liquid limit, PI: Plasticity index, MDD: Maximum dry density, OMC: Optimum moisture content, UCS: Unconfined compressive strength

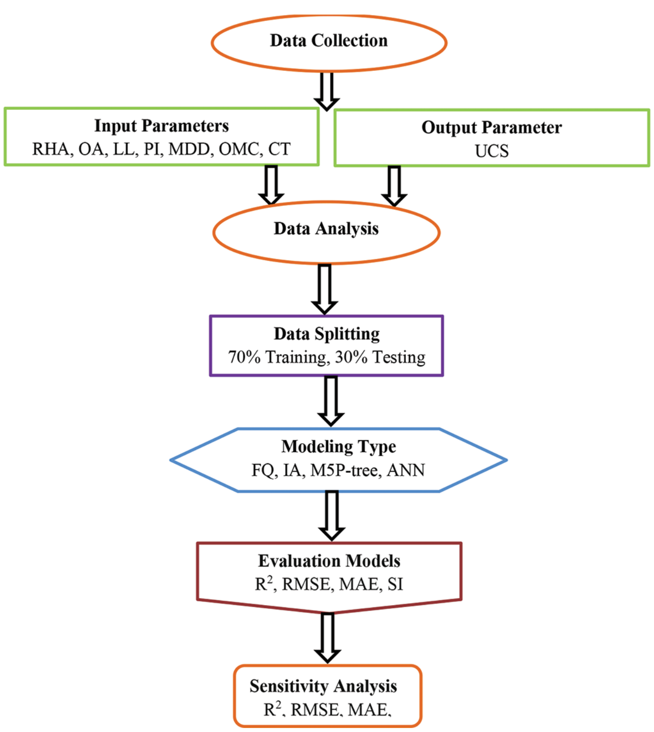

Fig. 1. The process of the work by a flow chart diagram.

developed based on input characteristics to estimate UCS. In the fifth stage, the models were evaluated based on testing data to establish their accuracy in predictions. Finally, in the sixth stage, sensitivity analysis was performed to determine the highest impact of input parameters.

IV. Correlations Between Input and Output Parameters

Figs. 2 and 3 showed the correlation and matrix plots between the input parameters and UCS values. Among all the parameters, CT showed a moderate positive relationship with UCS ($r = 0.58$). Other parameters, such as LL, PI, and dry density, showed weak or negative correlations. CT supports pozzolanic reactions in RHA-treated soil, resulting in cementitious products that increase strength. Insufficient curing causes incomplete reaction and reduced UCS. While LL and PI affect soil workability and water retention, they do not strongly correlate with UCS unless combined with density, moisture content, and CT.

Table II shows descriptive statistics for each variable. Kurtosis and skewness describe the form of a distribution. In numerical analysis, kurtosis denotes a distribution's peak

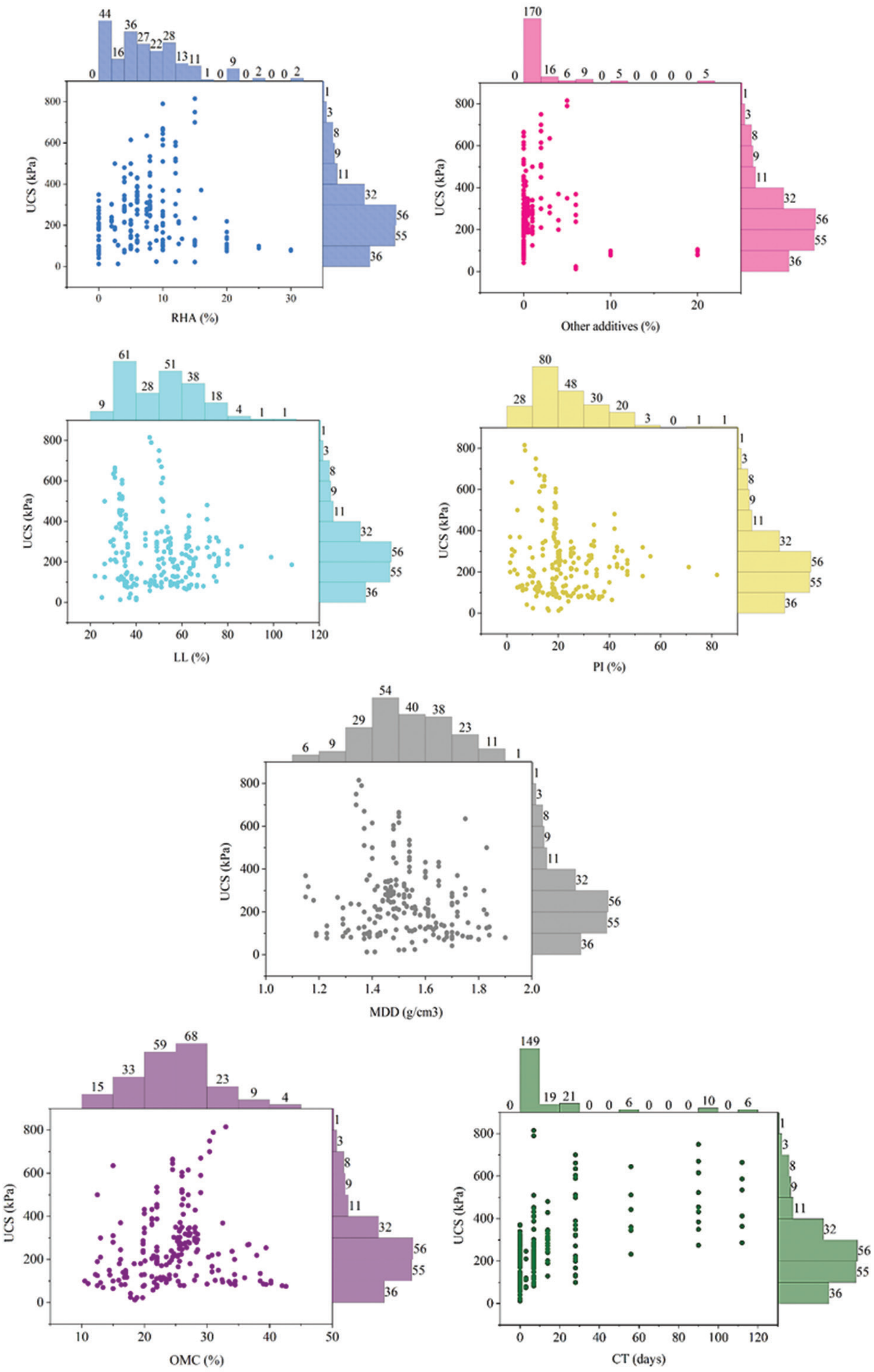

Fig. 2. Matrix plot between the input parameters and the unconfined compressive strength.

or flatness, whereas skewness refers to asymmetry. Negative kurtosis indicates shorter and thinner tails than normal distributions. A positive kurtosis value suggests lengthier and fatter tails than a normal distribution. Generally, a normal distribution has a kurtosis value of 0 (nearly zero in LL, MDD, and OMC). A distribution with high negative kurtosis may imply that there are lesser extreme values. Hence, input and output values should be chosen to avoid extreme distribution ends. A negative skewness number proposes a longer left tail, while a positive skewness value indicates a longer right tail. Similarly, LL, MDD, and OMC have the smallest values. This is illustrated in Figs. 2c, 2e, and 3f. Overall, negative skewness and kurtosis in MDD and OMC suggest that the dataset contains uniformly distributed soil properties with a tendency to higher values. This distribution helps consistent and predictable UCS outputs in fine-grained soils.

	RHA (%)	Additives (%)	LL (%)	PI (%)	MDD (g/cm^3)	OMC (%)	Curing time (days)	UCS (kPa)
RHA (%)	1							
Additives (%)	0.21	1						
LL (%)	−0.14	−0.03	1					
PI (%)	−0.29	−0.07	0.79	1				
MDD (g/cm^3)	−0.50	−0.26	−0.30	−0.14	1			
OMC (%)	0.49	0.24	0.38	0.32	−0.85	1		
Curing time (days)	−0.01	−0.13	−0.33	−0.16	0.03	−0.05	1	
UCS (kPa)	0.05	−0.12	−0.15	−0.16	−0.16	0.11	0.58	1

RHA: Rice husk ash, LL: Liquid limit, PI: Plasticity index, MDD: Maximum dry density, OMC: Optimum moisture content, UCS: Unconfined compressive strength

Fig. 3. Correlation matrix between the input and output parameters.

TABLE II
Statistical Measures for Input and Output Variables

	RHA (%)	OA (%)	LL (%)	PI (%)	MDD (g/cm^3)	OMC (%)	CT (days)	UCS (kPa)
Min	0	0	22	1.3	1.2	10.5	0	13.1
Max	30.0	20	108	82	1.9	42.6	112.0	815
Mean	6.9	1.4	50.3	22.4	1.5	24.4	14.6	249.8
Median	6.0	0	51	19.4	1.5	24.7	7	219
Mode	0.0	0	51	25	1.5	22	0	130
Variance	35.4	12.6	239.1	166.5	0	42.3	725.2	26521.4
Standard deviation	5.9	3.5	15.5	12.9	0.2	6.5	26.9	162.9
Skewness	1.1	3.9	0.4	1.1	0	0.3	2.5	1.2
Kurtosis	1.7	16.6	0.1	2.2	−0.2	0.2	5.2	1.2
Sum	1462.5	295	10611.3	4734	321.3	5141.1	3088	52699.8
Count	211	211	211	211	211	211	211	211

RHA: Rice husk ash, LL: Liquid limit, PI: Plasticity index, MDD: Maximum dry density, OMC: Optimum moisture content, UCS: Unconfined compressive strength, CT: Curing time

V. Modeling

This section evaluates the predictive performance of four models – FQ, IA, M5P-tree, and ANN – using standard metrics on the UCS dataset. Models are employed to forecast UCS, and their performance is assessed compared to the measured data using valuation standards, including proportion difference between investigated and predicted data, R^2 value, RMSE, MAE, and SI values. The least squares method is used in Excel and soft computing, such as WEKA to calculate parameter coefficients in all models. It includes minimizing the sum of squared variances between the observed data points and the predicted values of the line of best fit. Overall, the models show that non-linear correlations, IAs, and complicated variable dependencies must all be considered when predicting UCS (Vipulanandan et al., 2012).

A. FQ Model

The mathematical FQ model uses various input parameters to predict UCS values for natural and treated soils. This model can capture non-linear correlations between input parameters and UCS values (Ali, 2024; Hoque, et al., 2023; Meskini, et al., 2022; Wang, et al., 2023). The FQ model equation is as follows:

$$UCS = \beta_0 + \beta_1 * (RHA) + \beta_2 * (OA) + \beta_3 * (LL) + \beta_4 * (PI) + \beta_5 * (MDD) + \beta_6 * (OMC) + \beta_7 * (CT) + \beta_8 * (RHA * OA) + \beta_9 * (RHA * LL) + \beta_{10} * (RHA * PI) + \beta_{11} * (RHA * MDD) + \beta_{12} * (RHA * OMC) + \beta_{13} * (RHA * CT) + \beta_{14} * (OA * LL) + \beta_{15} * (OA * PI) + \beta_{16} * (OA * MDD) + \beta_{17} * (OA * OMC) + \beta_{18} * (OA * CT) + \beta_{19} * (LL * PI) + \beta_{20} * (LL * MDD) + \beta_{21} * (LL * OMC) + \beta_{22} * (LL * CT) + \beta_{23} * (PI * MDD) + \beta_{24} * (PI * OMC) + \beta_{25} * (PI * CT) + \beta_{26} * (MDD * OMC) + \beta_{27} * (MDD * CT) + \beta_{28} * (OMC * CT) + \beta_{29} * (RHA)^2 + \beta_{30} * (OA)^2 + \beta_{31} * (LL)^2 + \beta_{32} * (PI)^2 + \beta_{33} * (MDD)^2 + \beta_{34} * (OMC)^2 + \beta_{35} * (CT)^2 \quad (1)$$

The model parameters are defined as β_0–β_{35} values. The clarification of coefficients in the FQ model can be more composite than the multilinear linear regression model.

B. IA Model

IA multivariable models consider non-linear IAs among input and output parameters to predict UCS (Ahmed, et al., 2021; Ghafor, et al., 2022; Tahr, Mohammed, and Ali, 2022). The general equation for an IA multivariable model is as follows:

$$UCS = \beta_0 + \beta_1 * (RHA) + \beta_2 * (OA) + \beta_3 * (LL) + \beta_4 * (PI) + \beta_5 * (MDD) + \beta_6 * (OMC) + \beta_7 * (CT) + \beta_8 * (RHA * OA) + \beta_9 * (RHA * LL) + \beta_{10} * (RHA * PI) + \beta_{11} * (RHA * MDD) + \beta_{12} * (RHA * OMC) + \beta_{13} * (RHA * CT) + \beta_{14} * (OA * LL) + \beta_{15} * (OA * PI) + \beta_{16} * (OA * MDD) + \beta_{17} * (OA * OMC) + \beta_{18} * (OA * CT) + \beta_{19} * (LL * PI) + \beta_{20} * (LL * MDD) + \beta_{21} * (LL * OMC) + \beta_{22} * (LL * CT) + \beta_{23} * (PI * MDD) + \beta_{24} * (PI * OMC) + \beta_{25} * (PI * CT) + \beta_{26} * (MDD * OMC) + \beta_{27} * (MDD * CT) + \beta_{28} * (OMC * CT) \quad (2)$$

Model parameters range from β_0 to β_{28}. The IA term indicates that the impact of one interpreter variable on the output variable is dependent on the values of another predictor variable.

C. M5P-tree Model

Fig. 4 shows the M5P-tree analysis tree for input and output parameters in a geotechnical context, almost certainly related to

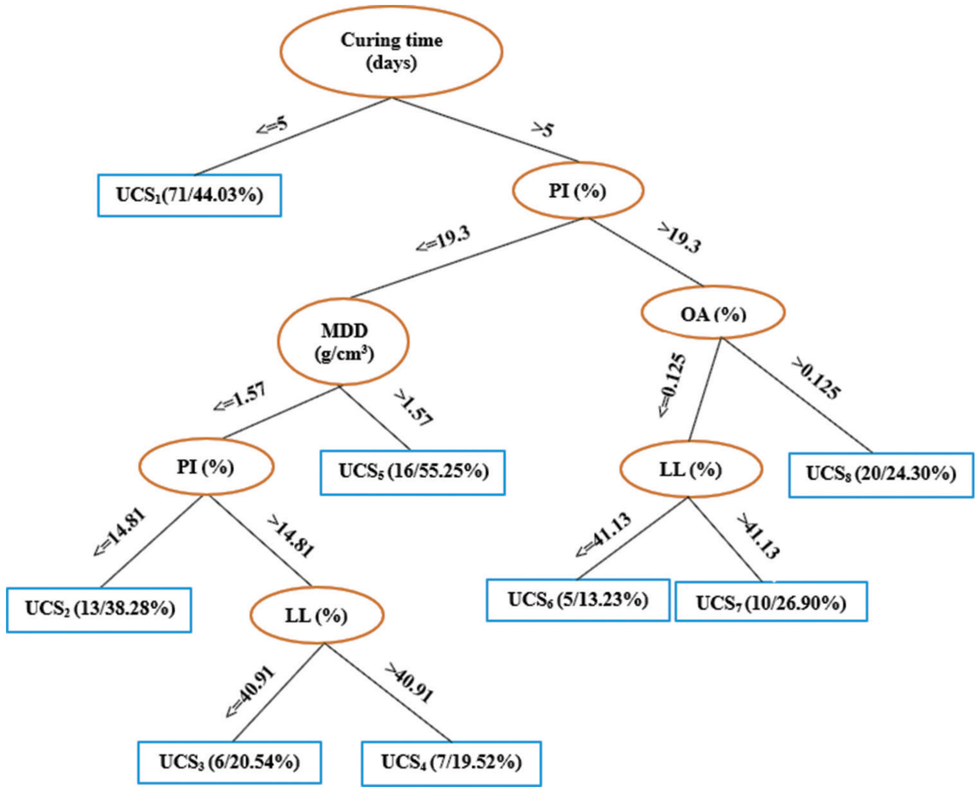

Fig. 4. M5P-tree analysis tree of input and output parameters.

soil stabilization using UCS values. The M5P-tree model offers both a logical structure for decision-making and the ability to model numerical data in a divided linear method. The UCS is organized into modules (UCS_1-UCS_8), with each branch corresponding to specific combinations of input parameters. In addition, this analysis reveals the complexities of parameters affecting soil strength and the systematic identification of their roles (Ahmad et al., 2022; Gnananandarao et al., 2022; Gnananandarao et al., 2023; Mahmood & Mohammed, 2022; Mohammed et al., 2020; Mohanty et al., 2019; Sihag et al., 2021; Suthar, 2020). The M5P-tree model equation is as follows:

$$UCS_1 = -6.56OA + 1.665LL - 0.412PI - 279.55MDD + 0.58CT + 525.78 \quad (3)$$

$$UCS_2 = 4.25RHA + 33.44OA - 4.40LL - 9.80PI - 294.66MDD + 2.39CT + 1032.67 \quad (4)$$

$$UCS_3 = -RHA + 22.41OA - 5.87LL - 9.80PI - 294.66MDD + 1.89CT + 1156.28 \quad (5)$$

$$UCS_4 = -1.54RHA + 22.41OA - 5.80LL - 9.80PI - 294.66MDD + 1.89CT + 1144.56 \quad (6)$$

$$UCS_5 = 11.25RHA + 9.65OA - 3.38LL - 0.39PI - 363.15MDD + 1.72CT + 913.91 \quad (7)$$

$$UCS_6 = 12.37OA - 1.20LL + 1.35PI - 88.77MDD + 1.21CT + 380.60 \quad (8)$$

$$UCS_7 = 12.37OA - 0.31LL + PI - 88.77MDD + 1.21CT + 333.294 \quad (9)$$

$$UCS_8 = -27.48OA + 0.27LL - 0.39\,PI - 88.77MDD + 7.85OMC + 3.65CT + 177.97 \quad (10)$$

D. ANN Model

ANN is an influential simulation program designed to process and analyze data evidence equally to a human brain. This mechanism learning technique is commonly used in construction engineering to predict how many numerical problems will behave in the future (Verma and Kumar, 2021; Wang and Huang, 1984). In this research, a multilayer feed-forward Network is assembled using proportions, weight/bias, and parameters (RHA, OA, LL, PI, MDD, OMC, and CT) as inputs, whereas the output ANN is the UCS values. There is no conventional method to structure Network architecture; the ideal network construction procedure includes selecting the optimal number of training periods to achieve low MAE and RMSE while maintaining a high R-value (Mohammed, et al., 2021; Sharma and Singh, 2018; Zeng, et al., 2021). Multiple transfer functions and ANN architectures with hidden layers and neurons were tested to optimize the Network structure and forecast UCS. Fig. 5 represents the best Network architectures for estimating UCS of natural and treated soils. Overall, the architecture of three hidden layers with six neurons per layer is likely a viable compromise to meet the problem's complexity while minimizing processing overhead.

VI. Model Valuation Tools

Model accuracy was assessed using R^2, RMSE, MAE, and SI, summarized in Table III and Figs. 6-9. ANN consistently outperformed others, while FQ and IA performed better in lower UCS ranges. The formulas below can be used to calculate the following metrics:

TABLE III
Comparative Analysis of Models Based on Ease of Use, Computational Efficiency, Interpretability and Accuracy

Models	Ease of use	Computational efficiency	Interpretability	Accuracy (R^2)
Full quadratic	High	High	High	Moderate
Interaction model	High	Moderate	Moderate	Moderate
M5P-Tree	Moderate	High	Moderate	High
ANN	Low (requires expertise)	Low	Low	Very high

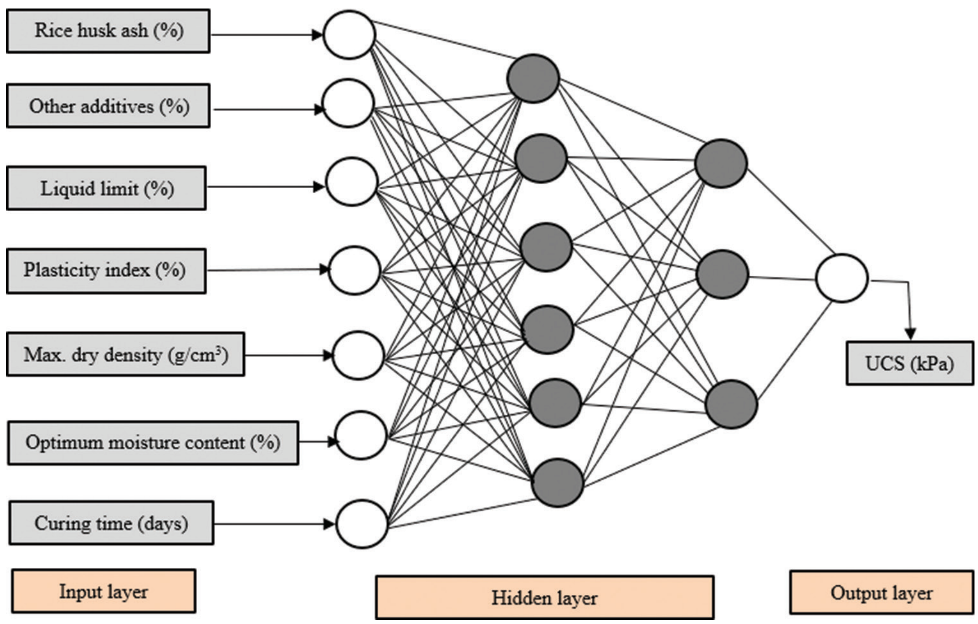

Fig. 5. The architecture of the used artificial neural network models and unconfined compressive strength.

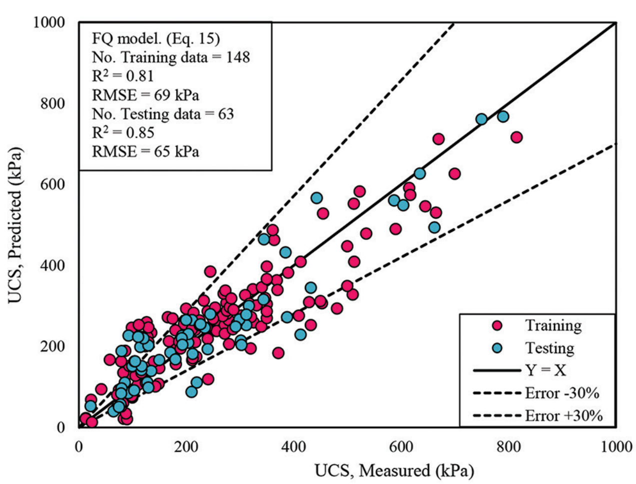

Fig. 6. Correlation between unconfined compressive strength and free swelling of natural and treated soil (Belabbaci, Mamoune, and Bekkouche, 2013).

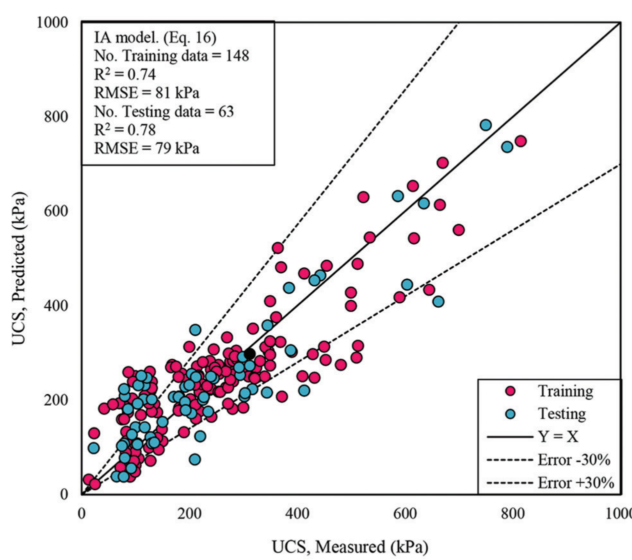

Fig. 7. The R2 values of unconfined compressive strength for all four models.

$$R^2 = \left(\frac{\sum_{p=1}^{p} (yi - yi')(yp - yp')}{\sqrt{\left[\sum_{P=1}^{P} (yi - yi')^2\right]\left[\sum_{P=1}^{P} (yi - yi')^2\right]}} \right)^2 \tag{11}$$

$$RMSE = \sqrt{\frac{\sum_{p=1}^{p} (yp - yi)^2}{p}} \tag{12}$$

$$MAE = \frac{\sum_{p=1}^{p} | yp - yi |}{p} \tag{13}$$

$$SI = \frac{RMSE}{y'} \tag{14}$$

VII. Results and Discussion

Table III presents a qualitative comparison of the models' accuracy, ease of use, and interpretability. Among

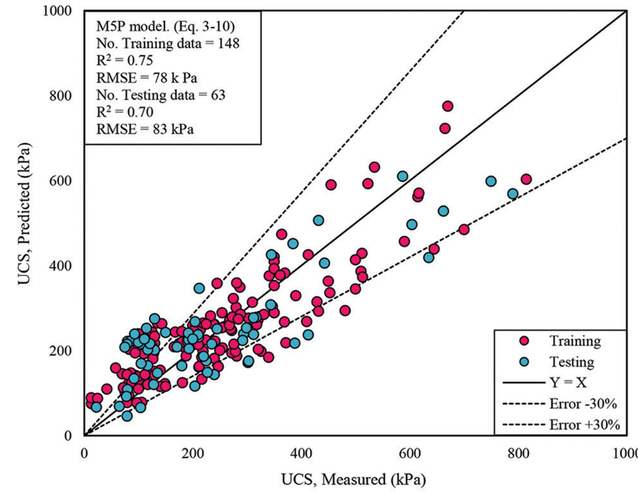

Fig. 8. The RMSE values of unconfined compressive strength for all four models.

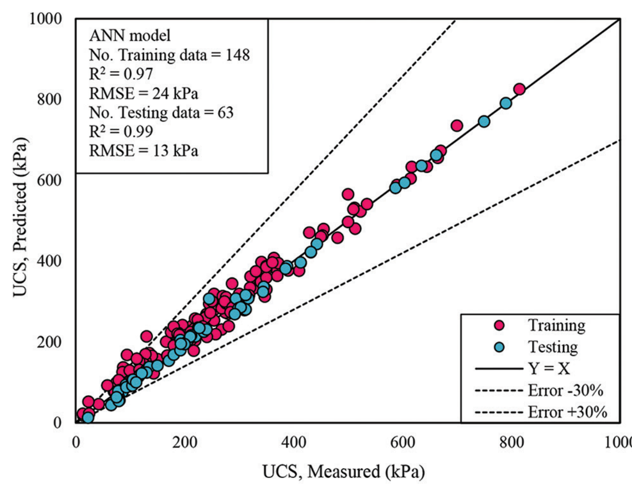

Fig. 9. The MAE values of unconfined compressive strength for all four models.

the evaluated models, the ANN approach demonstrated the highest predictive accuracy for UCS, outperforming M5P-tree, FQ, and IA models. While the FQ model was more interpretable, it lacked precision in nonlinear cases, which the ANN addressed effectively.

A. FQ Model

The FQ model achieved R^2 values of 0.81 (training) and 0.85 (testing) in predicting UCS. The training and testing datasets have RMSE values of 69 and 65 kPa, respectively. Fig. 10 compares the actual and expected UCS values. FQ provides equations incorporating linear, quadratic, and IA terms for input parameters. The coefficients in the equations represent how each parameter affects the result. Equation 15 shows UCS models with assigned weights for each parameter (Hama Ali, 2023; Li et al., 2021; Mawlood et al., 2022).

$$UCS = -3403.37 - 77.337RHA - 19.438OA - 28.439LL + 4.817PI + 2905.378MDD + 204.959OMC - 13.088CT + 0.917(RHA*OA) - 0.172(RHA*LL) + 0.035(RHA*PI) + 47.791(RHA*MDD) + 1.138(RHA*OMC) + 0.321(RHA*CT) + 1.172(OA*LL) -0.901(OA*PI) - 25.778(OA*MDD) + 0.181(OA*OMC) + 2.504(OA*CT) + 0.089(LL*PI) + 14.655(LL*MDD) + 0.275(LL*OMC) - 0.091(LL*CT) - 4.920(PI*MDD) + 0.133(PI*OMC) - 0.003(PI*CT) - 82.853(MDD*OMC) + 13.817(MDD*CT) + 0.003(OMC*CT) - 0.834(RHA)^2 - 0.216(OA)^2 - 0.003(LL)^2 - 0.112(PI)^2 - 681.150(MDD)^2 - 2.121(OMC)^2 + -0.050(CT)^2 \quad (15)$$

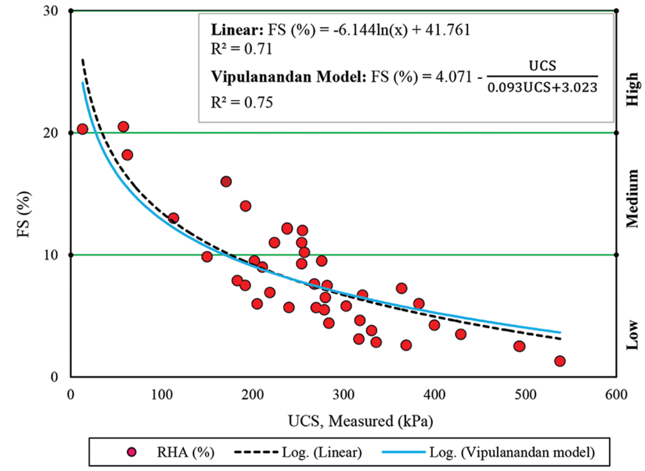

Fig. 10. Comparison between measured and predicted values of unconfined compressive strength for full quadratic model.

The parameters with a considerable positive effect on UCS are PI, MDD, and OMC, with coefficients of 4.8, 2905.4, and 205, respectively. RHA, OA, LL, and CT negatively affect UCS, with values of −77.3, −19.4, −28.4, and −13.1.

B. IA Model

Fig. 11 compares actual and predicted UCS values using the IA model. The IA model offered similar interpretability to the FQ but with slightly lower accuracy (R^2 = 0.74 training, 0.78 testing). In addition, the training and testing data have RMSEs of 81 and 79 kPa. Therefore, the IA model may yield a satisfactory prediction for UCS values (Ali & Mohammed, 2024; Ali et al., 2024; Eyo et al., 2022). Equation 16 shows the mathematical formula of the IA model for UCS.

$$UCS = -1007.088 - 1.391(RHA) + 0.021(OA) + 19.370(LL) + 37.216(PI) + 360.966(MDD) + 4.433(OMC) - 26.413(CT) + 0.930(RHA*OA) - 0.258(RHA*LL) + 0.704(RHA*PI) + 15.510(RHA*MDD) - 0.990(RHA*OMC) + 0.443(RHA*CT) + 1.232(OA*LL) - 1.015(OA*PI) - 31.099(OA*MDD) - 0.492(OA*OMC) + 1.817(OA*CT) + 0.086(LL*PI) - 11.081(LL*MDD) - 0.082(LL*OMC) + 0.029(LL*CT) - 18.231(PI*MDD) - 0.797(PI*OMC) + 0.017(PI*CT) + 18.769(MDD*OMC) + 14.153(MDD*CT) + 0.115(OMC*CT) \quad (16)$$

C. M5P Model

Fig. 12 depicts a scatter plot of measured and predicted UCS values for natural and treated soils, using an M5P model. It performed moderately well (R^2 = 0.75 training, 0.70 testing) but exhibited higher RMSE in predicting UCS >500 kPa. The figure shows ±30% error bands, indicating the model's

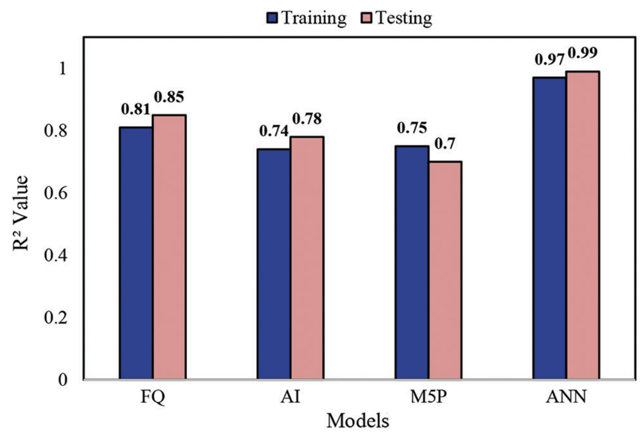

Fig. 11. Comparison between measured and predicted values of unconfined compressive strength for the interaction model.

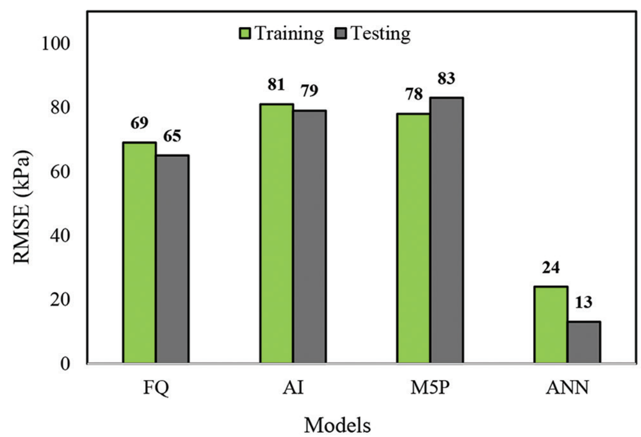

Fig. 12. Comparison between measured and predicted values of unconfined compressive strength for M5P model.

predicted accuracy. Most data points, particularly those with lower UCS values, fit inside these bands, indicating high model performance in this range. Points beyond the ±30% error range indicate considerable deviations between the model's predictions and actual results, especially for higher UCS values, which were similar to (Ahmad, et al., 2024; Ghanizadeh and Naseralavi, 2023; Pandey and Aggarwal, 2022; Sihag, Suthar, and Mohanty, 2021). The performance variance between training and testing data is small, implying that the M5P model generalizes reasonably well. Overall, while the M5P model displays satisfactory predictive capabilities with a low performance decrease between training and testing, improving the model for higher UCS values and experimenting with new modeling strategies may improve overall accuracy and strength.

D. ANN Model

Table IV compares various ANN designs to find the best model for UCS values. ANN using three hidden layers, six neurons on the left side (Fig. 5), 0.1 momentum, 0.1 learning rate, and 50000 iterations produces the best UCS prediction. Fig. 13 compares predicted and actual UCS values for training and testing datasets. The ANN model significantly outperformed all others in accuracy and generalizability. It achieved RMSE values of 24 kPa (training) and 13 kPa (testing), with minimal bias across the full UCS range. Similar results were achieved by (Ghorbani and Hasanzadehshooiili, 2018; Jalal, et al., 2021; Mohammed, Hummadi, and Mawlood, 2022; Pham, et al., 2021). The training and testing datasets for UCS have SI values of 0.1 and 0.07, respectively, as shown in Fig. 14. Also, the ANN model excels at predictive accuracy but faces limitations such as overfitting risks, computational complexity, reliance on massive datasets, low interpretability, and difficult hyperparameter tuning. Addressing these challenges through regulation, cross-validation, and simplified model integration can increase its practical applicability.

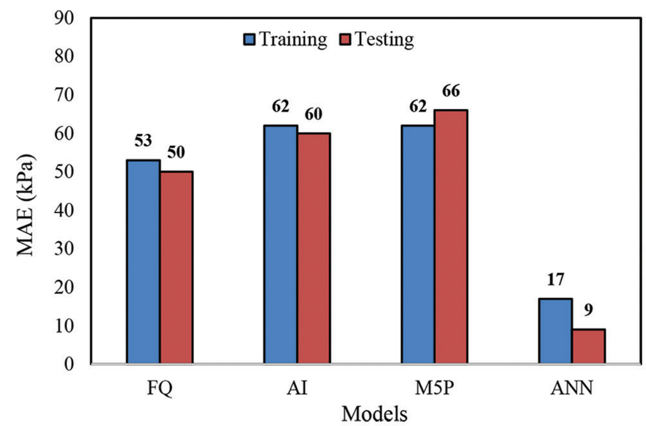

Fig. 13. Evaluation between measured and predicted values of unconfined compressive strength for artificial neural network model: training data and testing data.

TABLE IV
ANN Testing Architecture for UCS

No. of hidden layers	No. of neurons in hidden layers			R-Square	MAE (kPa)	RMSE (kPa)
	Left	Middle	Right			
1	3	0	0	0.78	55.58	70.68
1	5	0	0	0.84	43.39	59.57
1	6	0	0	0.82	46.69	63.72
1	8	0	0	0.88	35.47	52.05
1	9	0	0	0.89	36.36	47.77
2	5	0	5	0.94	25.77	37.01
2	6	0	6	0.94	25.75	48.20
2	7	0	7	0.96	21.78	30.46
3	**7**	**6**	**3**	**0.97**	**16.75**	**24.16**
3	7	5	2	0.96	17.65	28.08
3	5	4	2	0.93	35.41	46.35
3	5	5	5	0.91	32.28	43.47

Bold values indicate the best ANN model with highest R-square and lowest MAE and RMSE.

E. The Linear and Vipulanandan Correlations between UCS, and FS

Fig. 6 represents the relationship between UCS and swelling potential, as measured by the free swell index (FS). For both natural and RHA-treated soils, two models are used

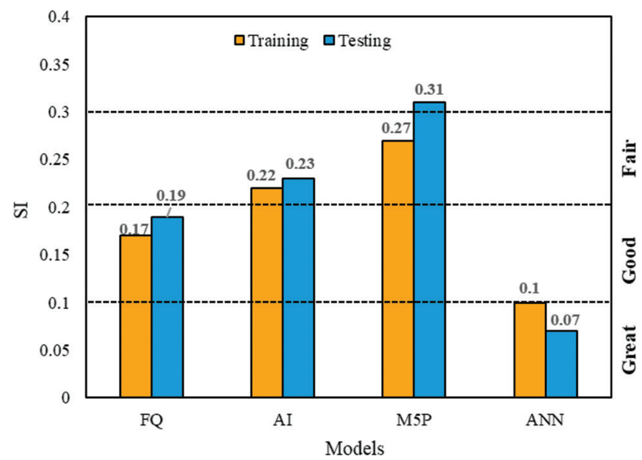

Fig. 14. The SI values of unconfined compressive strength for all four models.

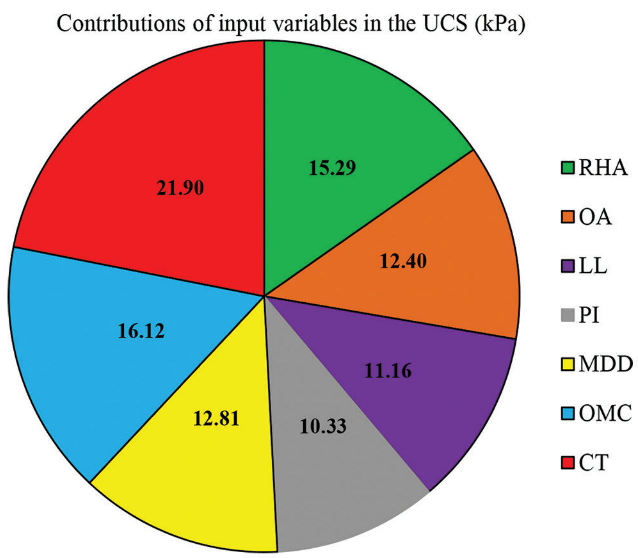

Fig. 15. The production of the sensitivity analysis for the main parameters' effect on the unconfined compressive strength.

to represent this relationship. The negative slope reveals an inverse relationship between UCS and FS, implying that as UCS increases, FS decreases. This suggests that stronger soil, as indicated by greater UCS values, has a reduced swelling potential, which is beneficial for the stabilization process. The R^2 value of 0.71 proposes a moderate to strong correlation, representing that the UCS describes 71% of the variance in FS in this linear model. Moreover, the Vipulanandan correlation model (2014) has an R^2 of 0.75, showing 75% of the variance in FS. The improved fit implies that the Vipulanandan model may better reflect the behavior of soil swelling as UCS changes, mainly at higher UCS values (Mawlood, et al., 2022; Mohammed, 2024; Rabat, Cano, and Tomás, 2020; Vipulanandan and Mohammed, 2020). Overall, The Vipulanandan model's higher R^2 value shows a more accurate depiction of the UCS-FS relationship for the natural and RHA-treated soils, specifically when predicting FS behavior is required. The linear and Vipulanandan correlation model equations are as follows:

$$FS\ (\%) = -6.144\ln(x) + 41.761\ \text{(Linear)} \tag{17}$$

$$FS\ (\%) = 4.071 - \frac{UCS}{0.093UCS + 3.023}\left(\text{Vipulanandan Model}\right) \tag{18}$$

VIII. Comparison Models

The study compares the employment of four multivariable models (FQ, IA, M5P, and ANN) in predicting UCS properties. The effectiveness of the models was assessed using four quantitative tools: R^2, RMSE, MAE, and SI, and the results were displayed in Figs. 7-9,14, respectively. These Figures show that the ANN model consistently outperformed others in all categories, particularly in reducing prediction error and residual spread The findings show that the ANN model has the greatest R^2 value for UCS in training (0.97) and testing (0.99) data sets, and the lowest RMSE values for UCS in training (24 kPa) and testing (13 kPa) data sets, followed by FQ, IA, and M5P models. In addition, SI measures data scatter about the regression line. Lower SI values recommend a better fit of the model to the data. The results show that the ANN model has the lowest SI values for UCS in training (0.1) and testing (0.07) data sets, followed by FQ, IA, and M5P models. Overall, Figs. 7-9,14 shows that while simpler models like FQ and IA offer interpretability, they fall short in generalizing over wide UCS ranges or under varying soil conditions.

IX. Sensitivity Analysis

A sensitivity analysis was performed to identify the most influential input variables affecting UCS predictions. The analysis employed a variable-exclusion approach: each input (RHA, OA, LL, PI, MDD, OMC, and CT) was individually removed, and changes in RMSE, R^2, and MAE were used to quantify its relative importance. The most comprehensive and precise model (the ANN model) was chosen to identify the parameter with the highest impact on UCS of natural and treated soils. The most common statistical measures (RMSE) were performed, as input parameter has a greater impact on RMSE values than other factors. Fig. 15 shows the results of the sensitivity analysis. The figure shows that CT had the highest influence (21.9%), followed by OMC (16.1%), RHA content (15.3%), MDD (14.3%), and PI (12.6%). The study found, when CT was excluded, the RMSE increased from 24 to 53 kPa. Excluding OMC or RHA content also caused significant accuracy losses, while LL and PI had marginal effects.

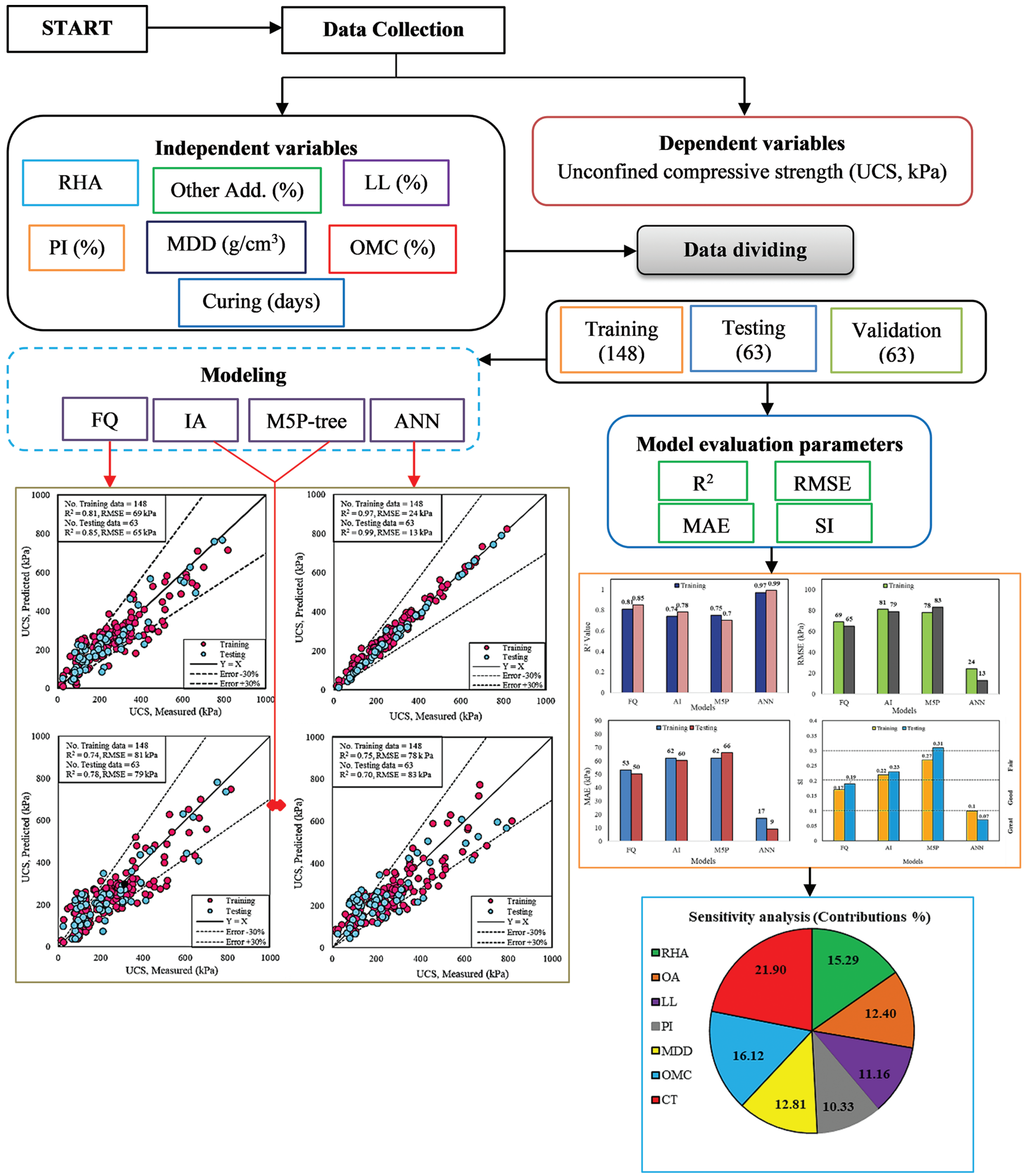

Fig. 16. Summary of the research framework and findings.

X. Conclusions

A. Findings

This study utilized various predictive models, including ANN and M5P-tree, along with FQ and IA, to predict the UCS of fine-grained soils stabilized with RHA. The overall modeling framework, comparative performance, and key findings are visually synthesized and provided in Fig. 16. The followings are the main findings of this study:

1. Out of the four models tested, the ANN gave the most accurate and reliable UCS predictions.
2. Both ANN and FQ models exhibited strong predictive performance for UCS, with SI values below 0.2. The IA model had fair accuracy with SI values between 0.2 and

0.3, while the M5P model showed weak accuracy with SI values of 0.3 and above.
3. The ANN model achieved the highest accuracy with an R^2 of 0.97, RMSE of 24 kPa, and MAE of 17 kPa, using inputs such as RHA, OA, LL, PI, MDD, OMC, and CT.
4. CT, OMC, and RHA content were the most important factors in predicting UCS.
5. ANN is great for accurate predictions but hard to interpret. FQ is more user-friendly because it provides clear equations.
6. Sensitivity analysis indicated that the CT (21.90%) had the biggest impact on UCS, followed by moisture content (16.12%) and RHA (15.29%).
7. Both the linear and Vipulanandan models demonstrated an inverse relationship between UCS and FS, showing that as UCS increases, FS decreases – indicating that stronger soils exhibit lower FS values

B. Research Limitations

1. The dataset involves 211 UCS test results, whereas wide may not fully capture the variability of soil structures across various topographical areas. A larger dataset integrating field-scale UCS tests would improve model generalizability.
2. The model was trained on laboratory-scale data and has not been validated in field conditions.
3. The study focuses on UCS prediction only; other parameters such as durability, swelling potential, or long-term behavior were not considered.
4. ANN models require computational resources and expertise, which may limit their direct application by practitioners without technical support.

C. Future Work Recommendations

1. Apply additional machine learning techniques, including ensemble models and deep learning, to boost accuracy and compare with traditional models such as M5P and ANN.
2. Study the durability and behavior of treated soils under varying environmental conditions over time.
3. Use soils with a wide range of LLs from different regions to enhance the model's adaptability and generalizability.
4. Perform large-scale real-world tests to confirm the reliability of ANN and other predictive models in actual geotechnical projects.

References

Abbey, S.J., Eyo, E.U., and Ng'ambi, S., 2020. Swell and microstructural characteristics of high-plasticity clay blended with cement. *Bulletin of Engineering Geology and the Environment*, *79*(4), pp.2119-2130.

Abdulrahman, S.M., Al-Kaream, A., Khalid, W., and Ihsan, E.A., 2024. Enhancing soil with low-cost pozzolanic materials: Rice husk ash and groundnut shell ash compared to cement. *Mathematical Modelling of Engineering Problems*, *11*(4), pp.1115-1122.

Adajar, M.A.Q., Aquino, C.J.P., Martin, C.P.H., and Urieta, D.K.G., 2019. Investigating the effectiveness of rice husk ash as stabilizing agent of expansive soil. *GEOMATE Journal*, *16*(58), pp.33-40.

Adhikary, S., and Jana, K., 2016. Potentials of rice husk ash as a soil stabilizer. *International Journal of Latest Research in Engineering and Technology*, *2*(2), pp.40-42.

Ahmad, M., Al-Mansob, R.A., Ramli, A.B.B., Ahmad, F., and Khan, B.J., 2024. Unconfined compressive strength prediction of stabilized expansive clay soil using machine learning techniques. *Multiscale and Multidisciplinary Modeling, Experiments and Design*, *7*(1), pp.217-231.

Ahmad, M., Alsulami, B.T., Al-Mansob, R.A., Ibrahim, S.L., Keawsawasvong, S., Majdi, A., and Ahmad, F., 2022. Predicting subgrade resistance value of hydrated lime-activated rice husk ash-treated expansive soil: A comparison between M5P, support vector machine, and gaussian process regression algorithms. *Mathematics*, *10*(19), p.3432.

Ahmed, A., 2013. Recycled bassanite for enhancing the stability of poor subgrades clay soil in road construction projects. *Construction and Building Materials*, *48*, pp.151-159.

Ahmed, C., Mohammed, A., and Saboonchi, A., 2022. ArcGIS mapping, characterisations and modelling the physical and mechanical properties of the Sulaimani City soils, Kurdistan Region, Iraq. *Geomechanics and Geoengineering*, *17*(2), pp.384-397.

Ahmed, H.U., Mohammed, A.S., and Mohammed, A.A., 2022. Multivariable models including artificial neural network and M5P-tree to forecast the stress at the failure of alkali-activated concrete at ambient curing condition and various mixture proportions. *Neural Computing and Applications*, *34*(20), pp.17853-17876.

Ahmed, H.U., Mohammed, A.S., Mohammed, A.A., and Faraj, R.H., 2021. Systematic multiscale models to predict the compressive strength of fly ash-based geopolymer concrete at various mixture proportions and curing regimes. *PLoS One*, *16*(6), pp.e0253006.

Alhassan, M., 2008. *Potentials of Rice Husk Ash for Soil Stabilization*. Available from: https://www.thaiscience.info/journals/article/aujt/10290698.pdf

Ali, H.F.H., 2024. Utilizing several multivariable mathematical and M5P-tree models to predict uniaxial compressive strength of rocks. *Multiscale and Multidisciplinary Modeling, Experiments and Design*, *7*(3), pp.1737-1753.

Ali, H.F.H., and Mohammed, A.S., 2024. Modeling the effect of chemical additives on clay soil plasticity: Novel analysis of oxide contributions in fly ash and cement treatments. *Modeling Earth Systems and Environment*, 10, pp.7049-7078.

Ali, H.F.H., Omer, B., Mohammed, A.S., and Faraj, R.H., 2024. Predicting the maximum dry density and optimum moisture content from soil index properties using efficient soft computing techniques. *Neural Computing and Applications*, *36*(19), pp.11339-11369.

Anupam, A.K., Kumar, P., and Ransingchung, R.N.G.D., 2014. Performance evaluation of structural properties for soil stabilised using rice husk ash. *Road Materials and Pavement Design*, *15*(3), pp.539-553.

Anwar Hossain Khandaker, M., 2011. Stabilized soils incorporating combinations of rice husk ash and cement kiln dust. *Journal of Materials in Civil Engineering*, *23*(9), pp.1320-1327.

Ashango, A.A., and Patra, N.R., 2014. Static and cyclic properties of clay subgrade stabilised with rice husk ash and Portland slag cement. *International Journal of Pavement Engineering*, *15*(10), pp.906-916.

Baghbani, A., Soltani, A., Kiany, K., and Daghistani, F., 2023. Predicting the strength performance of hydrated-lime activated rice husk ash-treated soil using two grey-box machine learning models. *Geotechnics*, *3*(3), pp.894-920.

Basha, E.A., Hashim, R., Mahmud, H.B., and Muntohar, A.S., 2005. Stabilization of residual soil with rice husk ash and cement. *Construction and Building Materials*, *19*(6), pp.448-453.

Behak, L., and Musso, M., 2016. Performance of low-volume roads with wearing course of silty sand modified with rice husk ash and lime. *Transportation Research Procedia*, *18*, pp.93-99.

Belabbaci, Z., Mamoune, S.M.A., and Bekkouche, A., 2013. Laboratory study of the influence of mineral salts on swelling (KCl, MgCl^ sub 2^). *Earth Science Research*, *2*(2), p.135.

Blayi, R.A., Omer, B., Sherwani, A.F.H., Hamadamin, R.M., and Muhammed, H.K., 2024. Geotechnical characteristics of fine-grained soil with wood ash. *Cleaner Engineering and Technology*, *18*, p.100726.

Blayi, R.A., Sherwani, A.F.H., Mahmod, F.H.R., and Ibrahim, H.H., 2021. Influence of rock powder on the geotechnical behaviour of expansive soil. *International Journal of Geosynthetics and Ground Engineering*, *7*(1), p.14.

Cabalar, A.F., and Omar, R.A., 2023. Stabilizing a silt using waste limestone powder. *Bulletin of Engineering Geology and the Environment*, *82*(8), p.300.

Canakci, H., Aziz, A., and Celik, F., 2015. Soil stabilization of clay with lignin, rice husk powder and ash. *Geomechanics and Engineering*, 8(1), pp.67-79.

Charyulu, S.V., Akhila, C., Vineetha, C., and Akanksha, A., 2023. Stabilisation of soil using rice husk ash (RHA) and cement. *E3S Web Conf.*, *391*, p.01201.

Choobbasti, A.J., Ghodrat, H., Vahdatirad, M.J., Firouzian, S., Barari, A., Torabi, M., and Bagherian, A., 2010. Influence of using rice husk ash in soil stabilization method with lime. *Frontiers of Earth Science in China*, *4*(4), pp.471-480.

Eberemu Adrian, O., Amadi Agapitus, A., and Sule, J., 2012. Desiccation effect on compacted tropical clay treated with rice husk ash. In: *Geo-Frontiers 2011*. Geo-Frontiers, Karnataka, pp. 1192-1201.

Emad, W., Salih Mohammed, A., Kurda, R., Ghafor, K., Cavaleri, L., Qaidi, S.M.A., Hassan, A.M.T., and Asteris, P.G., 2022. Prediction of concrete materials compressive strength using surrogate models. *Structures*, *46*, pp.1243-1267.

Estabragh, A.R., Moghadas, M., and Javadi, A.A., 2013. Effect of different types of wetting fluids on the behaviour of expansive soil during wetting and drying. *Soils and Foundations*, *53*(5), pp.617-627.

Eyo, E.U., Abbey, S.J., and Booth, C.A., 2022. Strength predictive modelling of soils treated with calcium-based additives blended with eco-friendly pozzolans-a machine learning approach. *Materials* (*Basel*), *15*(13), pp.4575.

Fattah, M.Y., Rahil, F.H., and Al-Soudany, K.Y., 2013. Improvement of clayey soil characteristics using rice husk ash. *Journal of Civil Engineering and Urbanism*, *3*(1), pp.12-18.

Gautam, N., Gupta Kritesh, K., Bhowmik, D., and Dey, S., 2023. Probing the stochastic unconfined compressive strength of lime-RHA mix treated clayey soil. *Journal of Materials in Civil Engineering*, *35*(3), p.04022469.

Ghafor, K., Ahmed, H.U., Faraj, R.H., Mohammed, A.S., Kurda, R., Qadir, W.S., Mahmood, W., and Abdalla, A.A., 2022. Computing models to predict the compressive strength of engineered cementitious composites (ECC) at various mix proportions. *Sustainability*, *14*(19), p.12876.

Ghanizadeh, A.R., and Naseralavi, S.S., 2023. Intelligent prediction of unconfined compressive strength and young's modulus of lean clay stabilized with iron ore mine tailings and hydrated lime using gaussian process regression. *Journal of Soft Computing in Civil Engineering*, *7*(4), pp.1-23.

Ghorbani, A., and Hasanzadehshooiili, H., 2018. Prediction of UCS and CBR of microsilica-lime stabilized sulfate silty sand using ANN and EPR models; application to the deep soil mixing. *Soils and Foundations*, *58*(1), pp.34-49.

Gnananandarao, T., Dutta, R.K., Khatri, V.N., and Kumar, M.S., 2022. Soft computing based prediction of unconfined compressive strength of fly ash stabilised organic clay. *Journal of Soft Computing in Civil Engineering*, *6*(4), pp.43-58.

Gnananandarao, T., Onyelowe, K.C., Dutta, R.K., and Ebid, A.M., 2023. Chapter sixteen - sensitivity analysis and estimation of improved unsaturated soil plasticity index using SVM, M5P, and random forest regression. In: Basetti, V., Shiva, C.K., Ungarala, M.R., and Rangarajan, S.S., Eds. *Artificial Intelligence and Machine Learning in Smart City Planning*. Elsevier, Netherlands, pp. 243-255.

Goktepe, A.B., Altun, S., Altintas, G., and Tan, O., 2008. Shear strength estimation of plastic clays with statistical and Neural approaches. *Building and Environment*, *43*(5), pp.849-860.

Hama Ali, H.F., 2023. Utilizing multivariable mathematical models to predict maximum dry density and optimum moisture content from physical soil properties. *Multiscale and Multidisciplinary Modeling, Experiments and Design*, *6*(4), pp.603-627.

Hoque, M.I., Hasan, M., Islam, M.S., Houda, M., Abdallah, M., and Sobuz, M.H.R., 2023. Machine learning methods to predict and analyse unconfined compressive strength of stabilised soft soil with polypropylene columns. *Cogent Engineering*, *10*(1), p.2220492.

Hossain, M.S., and Kim, W.S., 2015. Estimation of subgrade resilient modulus for fine-grained soil from unconfined compression test. *Transportation Research Record*, *2473*(1), pp.126-135.

Hossain, Z., Bulut, R., Tarhuni, F., and Al-Dakheeli, H., 2022. *Using Rice Husk Ash (RHA) as Stabilizing Agent for Problematic Subgrade Soils and Embankments*. Retrieved from: https://repository.lsu.edu/transet_pubs/141/

Ingabire, D., and Kumar, S., 2023. Enhancement of engineering properties of black cotton soil using rice husk and sawdust ash. *E3S Web Conf.*, *391*, p.01023.

Jalal, F.E., Mulk, S., Memon, S.A., Jamhiri, B., and Naseem, A., 2021. Strength, hydraulic, and microstructural characteristics of expansive soils incorporating marble dust and rice husk ash. *Advances in Civil Engineering*, *2021*(1), p.9918757.

Jalal, F.E., Xu, Y., Iqbal, M., Javed, M.F., and Jamhiri, B., 2021. Predictive modeling of swell-strength of expansive soils using artificial intelligence approaches: ANN, ANFIS and GEP. *Journal of Environmental Management*, *289*, p.112420.

Khan, R., Jabbar, A., Ahmad, I., Khan, W., Khan, A.N., and Mirza, J., 2012. Reduction in environmental problems using rice-husk ash in concrete. *Construction and Building Materials*, *30*, pp.360-365.

Kumar Yadav, A., Gaurav, K., Kishor, R., and Suman, S.K., 2017. Stabilization of alluvial soil for subgrade using rice husk ash, sugarcane bagasse ash and cow dung ash for rural roads. *International Journal of Pavement Research and Technology*, *10*(3), pp.254-261.

Li, C., Su, L., Liao, H., Zhang, C., and Xiao, S., 2021. Modeling of rapid evaluation for seismic stability of soil slope by finite element limit analysis. *Computers and Geotechnics*, *133*, pp.104074.

Lin, B., and Cerato, A.B., 2012. Prediction of expansive soil swelling based on four micro-scale properties. *Bulletin of Engineering Geology and the Environment*, *71*(1), pp.71-78.

Mahmood, W., and Mohammed, A., 2022. Performance of ANN and M5P-tree to forecast the compressive strength of hand-mix cement-grouted sands modified with polymer using ASTM and BS standards and evaluate the outcomes using SI with OBJ assessments. *Neural Computing and Applications*, *34*(17), pp.15031-15051.

Maithili, K.L., Nagakumar, M.S., and Shashishankar, A., 2024. Laboratory assessment of the effectiveness of rice husk ash, rice husk, and groundnut shells in soil improvement. *Indian Geotechnical Journal*, 54, pp.2143-2157.

Mawlood, Y., Mohammed, A., Hummadi, R., Hasan, A., and Ibrahim, H., 2022. Modeling and statistical evaluations of unconfined compressive strength and compression index of the clay soils at various ranges of liquid limit. *Journal of Testing and Evaluation*, *50*(1), pp.551-569.

Mawlood, Y., Salih, A., Hummadi, R., Hasan, A., and Ibrahim, H., 2021. Comparison of artificial neural network (ANN) and linear regression modeling with residual errors to predict the unconfined compressive strength and compression index for Erbil City soils, Kurdistan-Iraq. *Arabian Journal of Geosciences*, *14*(6), p.485.

McBratney, A.B., Odeh, I.O.A., Bishop, T.F.A., Dunbar, M.S., and Shatar, T.M., 2000. An overview of pedometric techniques for use in soil survey. *Geoderma*, *97*(3), pp.293-327.

Meskini, S., Remmal, T., Ejjaouani, H., and Samdi, A., 2022. Formulation and optimization of a phosphogypsum - fly ash - lime composite for road construction: A statistical mixture design approach. *Construction and Building Materials*, *315*, p.125786.

Mohammed, A., 2024. Property correlations and statistical variations in the geotechnical properties of (CH) clay soils. *Geotechnical and Geological Engineering*, *42*(1), p.843-858.

 http://dx.doi.org/10.14500/aro.11967

Mohammed, A., and Vipulanandan, C., 2015. Testing and modeling the short-term behavior of lime and fly ash treated sulfate contaminated CL soil. *Geotechnical and Geological Engineering*, *33*(4), pp.1099-1114.

Mohammed, A., Burhan, L., Ghafor, K., Sarwar, W., and Mahmood, W., 2021. Artificial neural network (ANN), M5P-tree, and regression analyses to predict the early age compression strength of concrete modified with DBC-21 and VK-98 polymers. *Neural Computing and Applications*, *33*(13), pp.7851-7873.

Mohammed, A., Hummadi, R.A., and Mawlood, Y.I., 2022. Predicting the chemical and mechanical properties of gypseous soils using different simulation technics. *Acta Geotechnica*, *17*(4), pp.1111-1127.

Mohammed, A., Rafiq, S., Sihag, P., Kurda, R., Mahmood, W., Ghafor, K., and Sarwar, W., 2020. ANN, M5P-tree and nonlinear regression approaches with statistical evaluations to predict the compressive strength of cement-based mortar modified with fly ash. *Journal of Materials Research and Technology*, *9*(6), pp.12416-12427.

Mohammed, A.S., 2018. Property correlations and statistical variations in the geotechnical properties of (CH) clay soils. *Geotechnical and Geological Engineering*, *36*(1), pp.267-281.

Mohanty, S., Roy, N., Singh, S.P., and Sihag, P., 2019. Estimating the strength of stabilized dispersive soil with cement clinker and fly ash. *Geotechnical and Geological Engineering*, *37*(4), pp.2915-2926.

Mousavi, S.M., Alavi, A.H., Gandomi, A.H., and Mollahasani, A.L.I., 2011. Nonlinear genetic-based simulation of soil shear strength parameters. *Journal of Earth System Science*, *120*(6), pp.1001-1022.

Mozumder, R.A., and Laskar, A.I., 2015. Prediction of unconfined compressive strength of geopolymer stabilized clayey soil using artificial neural network. *Computers and Geotechnics*, *69*, pp.291-300.

Muntohar, A.S., 2004. Utilization of uncontrolled burnt rice husk ash in soil improvement. *Civil Engineering Dimension*, *4*(2), pp.100-105.

Murty, V.R., and Praveen, G.V., 2008. Use of chemically stabilized soil as cushion material below light weight structures founded on expansive soils. *Journal of Materials in Civil Engineering*, *20*(5), pp.392-400.

Nahar, N., Owino, A.O., Khan, S.K., Hossain, Z., and Tamaki, N., 2021. Effects of controlled burn rice husk ash on geotechnical properties of the soil. *Journal of Agricultural Engineering*, *52*(4). Doi: 10.4081/jae.2021.1216

Nasir Amin, M., Iftikhar, B., Khan, K., Faisal Javed, M., Mohammad AbuArab, A., and Faisal Rehman, M., 2023. Prediction model for rice husk ash concrete using AI approach: Boosting and bagging algorithms. *Structures*, *50*, pp.745-757.

Ordoñez Muñoz, Y., Luis dos Santos Izzo, R., Leindorf de Almeida, J., Arrieta Baldovino, J., and Lundgren Rose, J., 2021. The role of rice husk ash, cement and polypropylene fibers on the mechanical behavior of a soil from Guabirotuba formation. *Transportation Geotechnics*, *31*, pp.100673.

Pandey, P.K., and Aggarwal, Y., 2022. ANN and M5P Approaches with Statistical Evaluations to Predict Compressive Strength of SCC Containing Silicas. In: *Proceedings of the International Conference on Paradigms of Communication, Computing and Data Sciences*, Singapore.

Pham, V.N., Huu-Dao, D., Erwin, O., and Ong, D.E.L., 2021. Prediction of unconfined compressive strength of cement-stabilized sandy soil in Vietnam using artificial neural networks (ANNs) model. *International Journal of Geotechnical Engineering*, *15*(9), pp.1177-1187.

Pushpakumara, B.H.J., and Mendis, W.S.W., 2022. Suitability of rice husk ash (RHA) with lime as a soil stabilizer in geotechnical applications. *International Journal of Geo-Engineering*, *13*(1), p.4.

Rabat, Á., Cano, M., and Tomás, R., 2020. Effect of water saturation on strength and deformability of building calcarenite stones: Correlations with their physical properties. *Construction and Building Materials*, *232*, p.117259.

Rahman, M.A., 1987. Effects of cement-rice husk ash mixtures on geotechnical properties of lateritic soils. *Soils and Foundations*, *27*(2), pp.61-65.

Rahman, M.D.A., 1986. The potentials of some stabilizers for the use of lateritic soil in construction. *Building and Environment*, *21*(1), pp.57-61.

Sarkar, G., Islam, M.R., Alamgir, M., and Rokonuzzaman, M., 2012. Interpretation of rice husk ash on geotechnical properties of cohesive soil. *Global Journal of Researches in Engineering Civil and Structural Engineering*, *12*(2), pp.1-7.

Sharma, L.K., and Singh, T.N., 2018. Regression-based models for the prediction of unconfined compressive strength of Artificially structured soil. *Engineering with Computers*, *34*(1), pp.175-186.

Sihag, P., Suthar, M., and Mohanty, S., 2021. Estimation of UCS-FT of dispersive soil stabilized with fly ash, cement clinker and GGBS by artificial intelligence. *Iranian Journal of Science and Technology, Transactions of Civil Engineering*, *45*(2), pp.901-912.

Suthar, M., 2020. Applying several machine learning approaches for prediction of unconfined compressive strength of stabilized pond ashes. *Neural Computing and Applications*, *32*(13), pp.9019-9028.

Tahr, Z., Mohammed, A., and Ali, J.A., 2022. Surrogate models to predict initial shear stress of clay bentonite drilling fluids incorporated with polymer under various temperature conditions. *Arabian Journal of Geosciences*, *15*(17), pp.1449.

Verma, G., and Kumar, B., 2021. Multi-layer perceptron (MLP) neural network for predicting the modified compaction parameters of coarse-grained and fine-grained soils. *Innovative Infrastructure Solutions*, *7*(1), p.78.

Vipulanandan, C., Ahossin Guezo, Y.J., and Bilgin, Ö., 2012. Geotechnical properties of marine and deltaic soft clays. In: *Advances in Measurement and Modeling of Soil Behavior*. United States: ASCE, pp.1-13.

Vipulanandan, C., and Mohammed, A., 2020. Characterizing the index properties, free swelling, stress-strain relationship, strength and compacted properties of polymer treated expansive CH clay soil using vipulanandan models. *Geotechnical and Geological Engineering*, *38*(5), pp.5589-5602.

Wang, M.C., and Huang, C.C., 1984. Soil compaction and permeability prediction models. *Journal of Environmental Engineering*, *110*(6), pp.1063-1083.

Wang, X., Kim, S., Wu, Y., Liu, Y., Liu, T., and Wang, Y., 2023. Study on the optimization and performance of GFC soil stabilizer based on response surface methodology in soft soil stabilization. *Soils and Foundations*, *63*(2), p.101278.

Wattanapanich, C., Imjai, T., Kefyalew, F., Aosai, P., Garcia, R., Vapppangi, S., and Noguchi, T., 2024. Integration of internet of things (IoT) and machine learning for management of ground water banks in drought-prone areas: A case study from imjai organic garden, Thailand. *Engineered Science*, *31*, p.1248.

Westerberg, B., Müller, R., and Larsson, S., 2015. Evaluation of undrained shear strength of Swedish fine-grained sulphide soils. *Engineering geology*, *188*, pp.77-87.

Yadu, L., Tripathi, R.K., and Singh, D., 2011. Comparison of fly ash and rice husk ash stabilized black cotton soil. *International Journal of Earth Sciences and Engineering*, *4*(6), pp.42-45.

Zaimoglu, A.S., 2015. Optimization of unconfined compressive strength of fine-grained soils modified with polypropylene fibers and additive materials. *KSCE Journal of Civil Engineering*, *19*(3), pp.578-582.

Zeng, J., Asteris, P.G., Mamou, A.P., Mohammed, A.S., Golias, E.A., Armaghani, D.J., Faizi, K., and Hasanipanah, M., 2021. The effectiveness of ensemble-neural network techniques to predict peak uplift resistance of buried pipes in reinforced sand. *Applied Sciences*, *11*(3), p.908.

Zhang, L., Liu, Z., Zhou, Y., Wu, T., and Sun, J., 2024. *Grounding Large Language Models in Real-World Environments using Imperfect World Models*. [Authorea Preprints].

Zivari, A., Siavoshnia, M., and Rezaei, H., 2023. Effect of lime-rice husk ash on geotechnical properties of loess soil in Golestan province, Iran. *International Journal of Geo-Engineering*, *14*(1), p.20.